

Exceedance probability as a tool to evaluate the wind environment of urban areas

Mahmoud Bady*

*Graduate School of Engineering, The University of Tokyo, 4-6-1 Komaba,
Meguro-ku, Tokyo, 153-8505, Japan*

Shinsuke Kato, Yoshihiro Ishida, Hong Huang and Takeo Takahashi

*Institute of Industrial Science, The University of Tokyo, 4-6-1 Komaba,
Meguro-ku, Tokyo, 153-8505, Japan*

(Received March 11, 2008, Accepted November 3, 2008)

Abstract. The present study aims to estimate the wind ventilation performance for pedestrian level domains from the air quality point of view. Three typical models of a dense urban area were considered and numerically simulated in order to examine the effects of the geometry of such models on wind flow characteristics, which in turn affect the air quality, within the pedestrian domain of a street canyon located within this area. The calculated flow fields were employed to estimate the exceedance probabilities within the study domain using a new approach: air exchange rate within the domain. The study has been applied to nine cities in Japan: Tokyo, Osaka, Sapporo, Niigata, Fukuoka, Nagoya, Sendai, Yokohama, and Kyoto, based on their mean wind velocity data. The results demonstrated that the exceedance probability analysis of the pedestrian wind environment could be a valuable tool during the design stage of inhabited areas for the evaluation of pollutant-removal efficiency by the applied wind. Also, the calculated probabilities demonstrated substantial dependence on both the geometry of building arrays and the wind conditions of the nine cities.

Keywords: exceedance probability; air exchange rate; urban ventilation; wind environment; built-up area.

1. Introduction

During the design stage for populated areas, it is quite important to assess the wind conditions at ground level, since these control the air quality within the pedestrian domains of such areas. The pedestrian wind conditions may strongly affect the dispersion of pollutants around buildings at the pedestrian level. Consequently, demonstration of a satisfactory wind environment is required to ensure a reasonable level of air quality for inhabitants (Richards, *et al.* 2002). From this perspective, the present research sheds light on how to analyze pedestrian wind environments within dense urban areas through the application of exceedance probability to assess the wind conditions of such areas.

* Corresponding Author, E-mail: mbady@iis.u-tokyo.ac.jp

Many researchers have studied wind conditions in urban areas and used the exceedance probability analysis to assess the safety and regular wind discomfort in such areas. Most of these studies focused on pedestrian-level winds. Melbourne (1978) studied assessment of prospective environmental wind conditions regarding a proposed building development in Australia. He described a method for predicting the probability of occurrence of a given wind speed at a particular location. Murakami, *et al.* (1986) constructed criteria for assessing wind conditions on the basis of wind speed and survey of residents' opinions over a long period of time. They used the exceedance probability analysis based on the Weibull distribution to describe their criteria, and they applied such criteria in evaluating the wind conditions in a typical city center area. Ohba, *et al.* (1998) carried out actual field measurements in order to study wind conditions at ground level around a redevelopment area in Tokyo. They used 17 measurement points to assess whether the wind conditions were acceptable or not based on three published criteria: Murakami (1978), Melbourne (1978) and Davenport, *et al.* (1975). Their study results demonstrate that Murakami's criterion is midway between those of Melbourne and Davenport. Similar to the previous study, Ratcliff and Peterka (1990) carried out wind tunnel measurements of pedestrian wind speeds for nine building projects to evaluate five different criteria using exceedance probability. Visser and Cleijne (1994) carried out wind tunnel experiments and full scale measurements to predict the wind climate around two buildings through the application of the exceedance probability approach. Murakami, *et al.* (1983) conducted observations of wind flow at ground level over a period of 2 years around a high-rise apartment building in a built-up area in Tokyo. They derived approximation of the exceedance probability for mean wind velocity and gust wind velocity at ground level by the Weibull distribution and they concluded that the approximation by the Weibull distribution becomes more accurate if the wind data for each wind direction is approximated separately and then those distributions are summed up. As an overview of previous studies, Stathopoulos (2006) addressed experimental and computational evaluations of the wind on people in an urban environment and focused on the development of human outdoor comfort criteria by considering a wide range of parameters, including wind speed, air temperature, relative humidity, solar radiation, air quality, human activity, clothing level, age and the like. He described an approach for establishing an overall comfort index taking into account, in addition to wind speed, the temperature and relative humidity in the urban area under consideration. Blocken, *et al.* (2004) carried out numerical simulations in order to assess the wind climate in the passages of three high-rise residential buildings in the city of Antwerp, Belgium. They found that the wind climate is highly unacceptable and accordingly, the authors have designed and analyzed an automatic control system to modify the wind climate in the passages. The exceedance probability was used not only for the assessment of wind climate but also -and especially- for the analysis of the automatic control system. In another study by Blocken and Carmeliet (2008), the exceedance probability was employed to assess the wind comfort at outdoor platforms for different design modifications of a high-rise apartment building. Based on their study, structural remedial measures for the considered building succeeded to bring the discomfort probability estimates down to acceptable levels.

From the above overview, it is demonstrated that there is only one approach for estimating the exceedance probability, i.e., wind velocity. In this paper, the exceedance probability was introduced via a new approach: air exchange rate (*AER*), as a reflection of the air quality of the considered domain. The new approach is introduced based on the fact that the air exchange rate is proportional to the wind velocity. Moreover, the previous work demonstrated that the calculation of exceedance probability was carried out based on the velocity at one point located within the study domain,

while it is very important to consider the entire volume of the pedestrian domain. The present paper takes this issue into account.

In order to carry out this study, firstly, computational fluid dynamics (CFD) simulations were performed in order to calculate the flow fields within the wind environment. An extensive amount of wind tunnel experiments were carried out in the same time to measure wind velocities and pollutant concentrations along the sides of the street domain for different geometries and different wind directions, Bady, *et al.* (2008). Then, the calculated flow fields were evaluated by comparing numerical and experimental data for wind velocity and gas concentrations within the street domain. Secondly, the calculated flow fields were employed to estimate air exchange rates within the pedestrian domain of the street. Thirdly, the exceedance probability was calculated for nine cities in Japan, namely Tokyo, Osaka, Sapporo, Niigata, Fukuoka, Nagoya, Sendai, Yokohama, and Kyoto, based on their mean wind velocity data.

2. Model description

Three typical models of a densely built-up area are illustrated in Fig. 1, and the geometry of the central part of model (I) is shown in Fig. 2. In Fig. 1, the white blocks express detached houses, while the grey area represents traffic roads and voids between adjacent buildings. The study domain (in all of these models) is the pedestrian volume located along a street surrounded by type-A and type-B blocks (shown in Fig. 2) and a fence of 1.5 m height around these blocks. The study domain has the same dimensions as the street ($40 \text{ m} \times 4 \text{ m}$) and extends to a height of 5.5 m.

Models (I), (II), and (III) have the same building arrangements and dimensions, but they differ in the geometry of the central part which surrounds the street (marked with black dashed lines). In model (I), the central part consists of eight type-A and two type-B blocks. Narrow gaps of 1 m width exist between the types-A buildings, and also between the type-B buildings. In model (II), the central part forms a solid U-shape. With respect to model (III), the street buildings are the same as those of model (I), while the outer blocks which surround them form a solid U-shape.

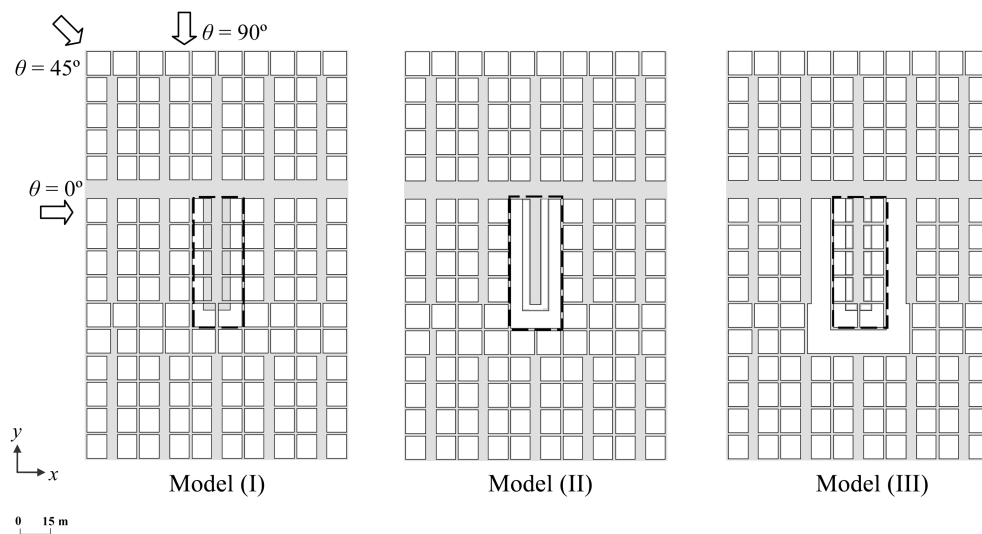


Fig. 1 Simplified diagrams for the three typical models of a dense urban area

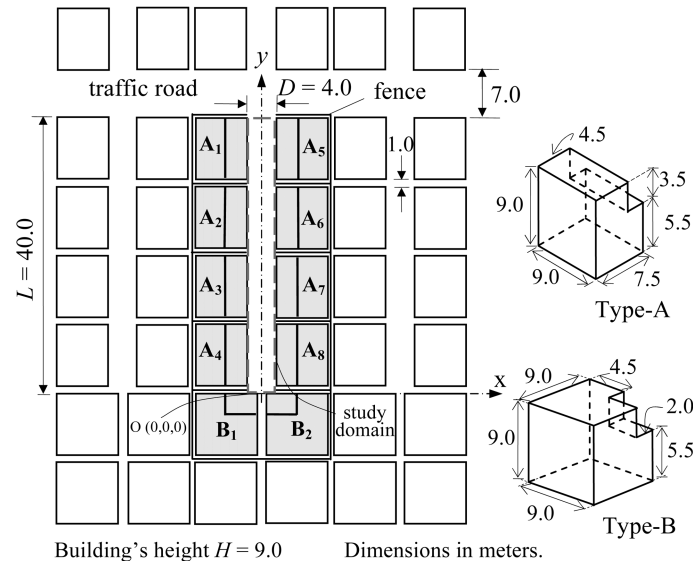


Fig. 2 Street characteristics in the case of model (I)

Many factors were born in mind during the design of these three building patterns. First, these models suit the nature of existing small-lot residential areas in Japan, as demonstrated by Katsumata (2004). Second, the three models were nominated to examine the optimum design for densely inhabited areas, which will induce more wind inside urban domains and will improve their air quality. Third, model (II) represents an unfavorable choice for dense urban areas, due to the blocking effect of its geometry in some wind directions. The U-shape of the central part of such model decelerates the wind motion and hence traps pollutants within the pedestrian domain of the street. Fourth, model (I) represents a spatially uniform-building array. Fifth, model (III) exhibits a combination between models (I) and (II), and as a result, it is expected to demonstrate behavior between these two models.

3. Methodology

As previously mentioned, the exceedance probability is introduced in this paper via air exchange rate, as a reflection of air quality of the considered domain. This approach is introduced based on the fact that air exchange rate is proportional to the wind velocity.

3.1. Air exchange rate

Air exchange rate represents the rate at which the total volume of air within the study domain is replaced with fresh air. It is calculated by dividing purging flow rate (PFR) by the volume of the corresponding domain:

$$AER = \frac{PFR}{V_p} \times 1000 \quad (1)$$

where, PFR is the purging flow rate (m^3/s), V_p is the domain volume (m^3) and p refers to pedestrian.

Purging flow rate is defined as the effective airflow rate required to purge/remove the pollutants from such domain (Bady, *et al.* 2008, Huang, *et al.* 2006). In other words, *PFR* represents the rate by which pollutants are flushed out of the domain, which represents the removal capacity by the wind from the domain. Purging flow rate is estimated using the concept of passive pollutants, which means that the flow field is not influenced by the pollutants. This makes it possible to calculate the flow field first, and then the calculated flow field is used to estimate *PFR*. The following Eq. (2) is used to calculate *PFR* (Bady, *et al.* 2008 and Huang, *et al.* 2006):

$$PFR = \frac{q_p}{c_p \times \rho} \quad (2)$$

where q_p denotes the pollutant generation rate (kg/s), ρ is the air density (kg/m³), and c_p is the domain's average concentration (kg/kg).

It is important to mention that *PFR* can be defined for a source point, not for the whole domain, but in this study, it is defined as common to the domain. Moreover, in addition to average concentrations, *PFR* can be estimated using the peak concentration of the domain. In such cases, the calculated *PFR* reflects dilution properties more than removal properties. In this study, purging flow rate is used to evaluate the air quality of the study domain.

3.2. Exceedance probability

The exceedance probability is a measure of the ventilation performance of the applied wind within a certain urban domain. It is described by the Weibull distribution which, for any azimuth direction a_n (i.e. $a_0 = N$, $a_1 = NNE \dots a_{15} = NNW$), is expressed as (Murakami, 1986 and Ohba, *et al.* 1998):

$$P(V_{exceed} > V_g) = A(a_n) \times \exp\left\{-\left(\frac{V_g}{C(a_n)}\right)^{K(a_n)}\right\} \quad (3)$$

In Eq. (3); $P(V_{exceed} > V_g)$ is the probability of exceeding a reference velocity V_g (shown in Fig. 3), $A(a_n)$ is the relative frequency of occurrence, and $C(a_n)$ and $K(a_n)$ are Weibull parameters for each wind direction.

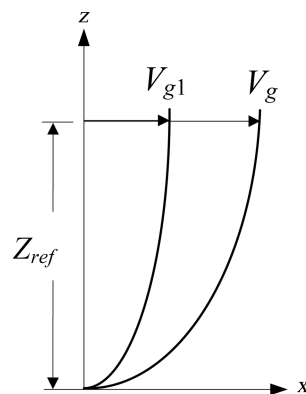


Fig. 3 Definition of V_g and V_{g1}

Eq. (3) is used to estimate the exceedance probability at the considered reference height. In order to calculate the probability at ground level, the following procedure is applied: a reference velocity referred to as V_{g1} , as illustrated in Fig. 3, is introduced. For such velocity, the air exchange rate within the study domain is calculated through CFD simulations to be AER_{g1} . The velocity V_g represents any reference velocity at the same height and the calculated air exchange rate at such velocity is AER_g . Since the wind velocity is proportional to the air exchange rate, then:

$$V_g = \frac{AER_g}{AER_{g1}} V_{g1} \quad (4)$$

Substituting Eq. (4) into Eq. (3), gives:

$$P\left(V_{exceed} > \frac{AER_g}{AER_{g1}} V_{g1}\right) = A(a_n) \times \exp\left\{-\left(\frac{AER_g}{AER_{g1} \times C(a_n)} V_{g1}\right)^{K(a_n)}\right\} \quad (5)$$

Rearranging the above Eq. (5) to get:

$$P\left(\frac{V_{exceed}}{V_{g1}} AER_{g1} > AER_g\right) = A(a_n) \times \exp\left\{-\left(\frac{AER_g}{AER_{g1} \times C(a_n)} V_{g1}\right)^{K(a_n)}\right\} \quad (6)$$

By defining AER_{exceed} to be:

$$AER_{exceed} = \frac{V_{exceed}}{V_{g1}} AER_{g1} \quad (7)$$

So, the exceedance probability based on air exchange rate for any wind direction a_n is:

$$PAE(R_{exceed} > AER_g) = A(a_n) \times \exp\left\{-\left(\frac{AER_g}{AER_{g1} \times C(a_n)} V_{g1}\right)^{K(a_n)}\right\} \quad (8)$$

where $P(AER_{exceed} > AER_g)$ is the probability of exceeding a reference air exchange rate AER_g .

In order to calculate the total exceedance probability for all directions, integration of Eq. (8) from 0° to 360° is required. It is an easy task if the integration is done manually using a coarse sector of 22.5° . In this case, there will be sixteen wind directions (i.e. $i = 0, 1 \dots 15$) and the final eq. becomes:

$$P(AER_{exceed} > AER_g) = \sum_{n=0}^{15} A(a_n) \times \exp\left\{-\left(\frac{AER_g}{AER_{g1} \times C(a_n)} V_{g1}\right)^{K(a_n)}\right\} \quad (9)$$

Fig. 4 illustrates the procedure for calculating the exceedance probability. For each one of the 16 directions of the building array ($i = 0 \sim 15$), there are sixteen wind directions ($n = 0 \sim 15$). This means that in order to estimate the total exceedance probability in all wind directions, 256 cases must be dealt with for every building model. In Fig. 4, the case of an array direction of ENE is illustrated as an example. In such case, the array is set at ENE direction while the incident wind direction is varied from N ($i = 13$) to NNW ($i = 12$) in a clockwise rotation with steps of 22.5° .

In this study, nine Japanese cities were selected to conduct the exceedance probability calculations on. These cities are Tokyo, Osaka, Sapporo, Niigata, Fukuoka, Nagoya, Sendai, Yokohama, and

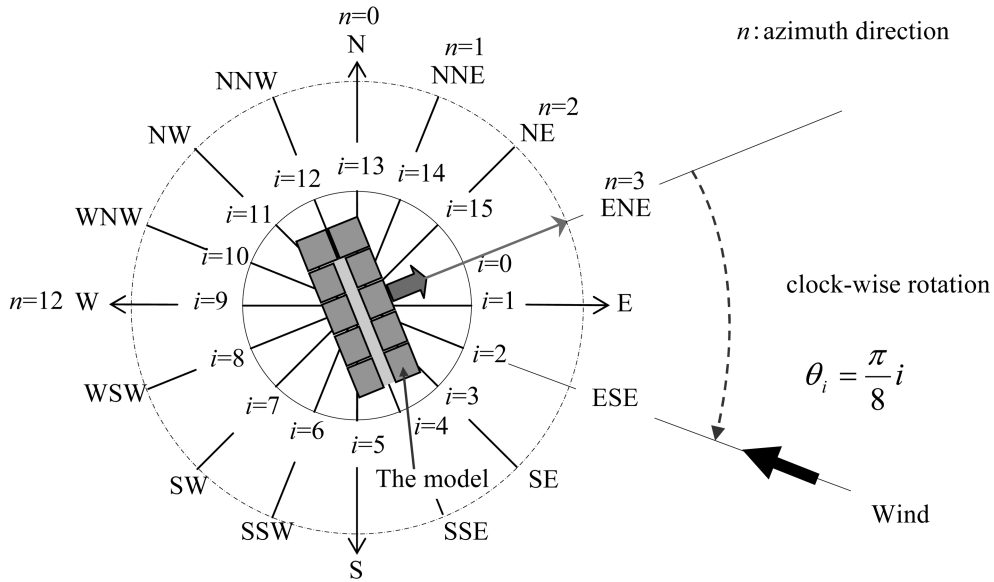
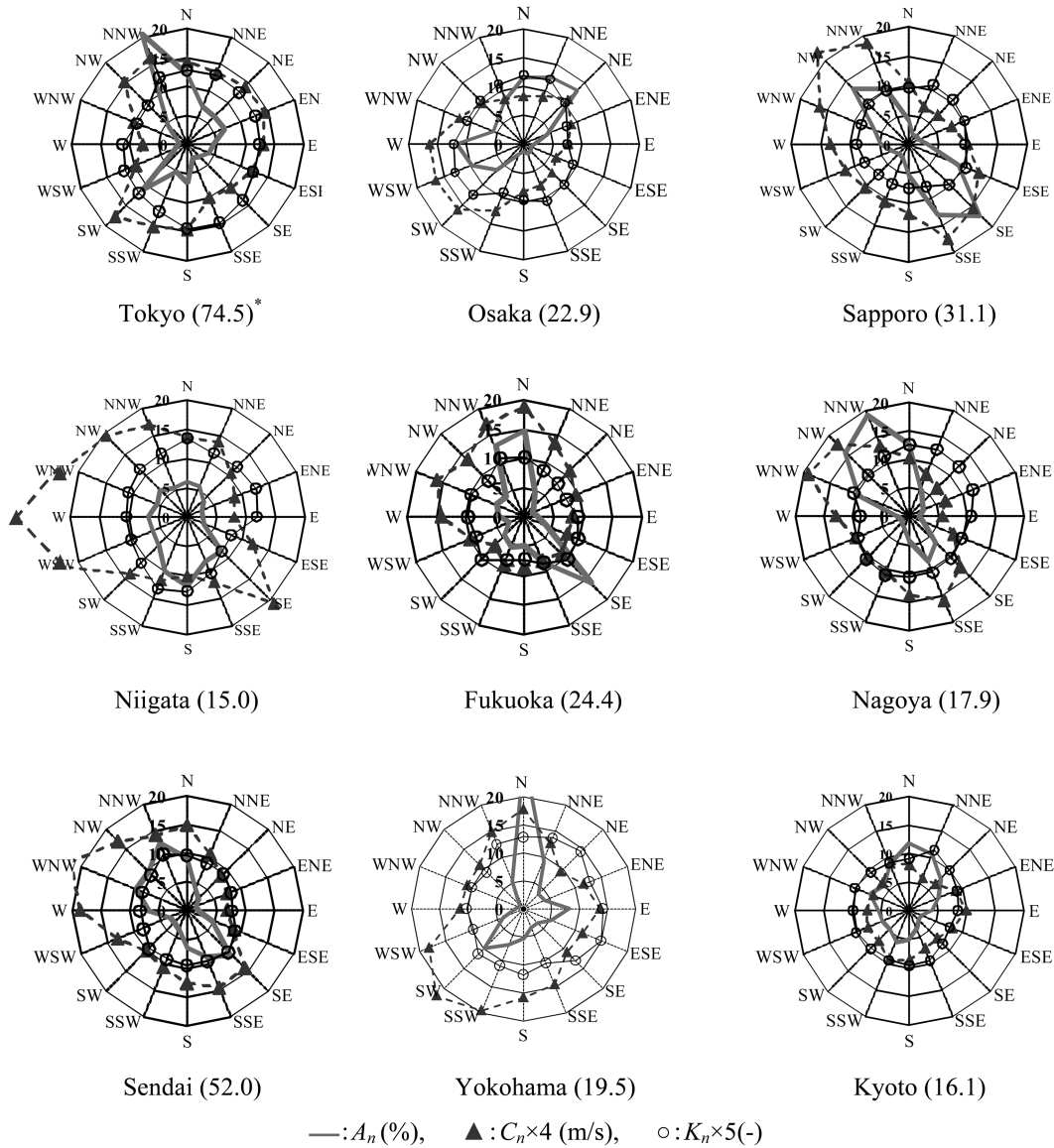


Fig. 4 Explanation of the method for calculating the exceedance probability



Fig. 5 Map of Japan showing the nine assessed cities

Kyoto. Fig. 5 presents a map of Japan showing the nine cities. The selection of these cities was based mainly on the fact that these cities are the most important cities in Japan, representing a significant proportion of the Japanese population and the site of many residential houses. In addition, these cities cover Japan from north to south, stretching from Sapporo to Fukuoka, which



* The numbers in brackets refer to the observation height in meters.

Fig. 6 Wind roses of the nine cities based on mean wind velocity (averaged over 10 minutes) (Murakami 1986)

means that the calculations of the exceedance probabilities for the nine selected cities will also be useful for other cities located nearby. Another important feature of the selected cities is that they have different characteristics, with some being coastal cities (both along the Sea of Japan and the Pacific Ocean) and others inland cities (i.e. such as Kyoto), and the wind regimes in coastal regions are different from those of inland areas. These reasons make the investigation of wind characteristics of such cities very important to ensure a reasonable level of air quality for the inhabitants of these cities.

Table 1 Weibull parameters for the 16 azimuth directions in the nine selected Japanese cities (Wind Engineering Institute of Japan 2005)

City	Parameter	NNE	NE	ENE	E	ESE	SE	SSE	S	SSW	SW	WSW	W	WNW	NW	NNW	N
Tokyo (74.5 m)*	A(a _n)	7.0%	6.7%	7.0%	4.6%	3.9%	2.9%	2.3%	6.6%	5%	11%	2.4%	1.5%	1.7%	4.8%	20.6%	12%
	C(a _n)	3.34	3.52	3.6	3.28	3.02	2.64	2.48	3.67	3.85	4.39	2.39	1.92	2.48	3.82	4.06	3.58
	K(a _n)	2.61	2.53	2.55	2.50	2.46	2.71	2.92	2.91	2.50	2.37	2.35	2.23	1.88	1.91	2.51	2.57
Osaka (22.9 m)	A(a _n)	12.6%	13.3%	4.4%	2.0%	1.4%	1.7%	1.9%	1.4%	1.9%	6.3%	9.8%	11.6%	5.6%	6.1%	8.2%	11.7%
	C(a _n)	2.24	2.74	2.24	1.94	1.53	1.75	1.95	2.06	3.14	4.03	4.10	4.06	2.99	2.52	2.12	2.08
	K(a _n)	2.43	2.04	1.62	1.52	1.85	1.98	2.13	1.94	1.81	2.46	2.57	2.42	2.12	2.13	2.26	2.40
Sapporo (31.1 m)	A(a _n)	1.8%	1.9%	1.9%	3.2%	9.0%	17.0%	12.8%	5.2%	2.6%	2.3%	3.0%	4.8%	6.4%	13.4%	10.2%	4.1%
	C(a _n)	1.70	1.73	1.97	2.50	3.23	3.86	4.36	2.97	2.65	2.62	2.92	3.32	4.09	5.49	4.62	2.62
	K(a _n)	2.17	2.11	2.05	1.91	2.11	1.94	1.55	1.50	1.46	1.46	1.63	1.78	1.74	1.92	1.97	1.90
Niigata (15.0 m)	A(a _n)	5.7%	3.9%	2.7%	2.7%	3.1%	8.3%	8.2%	11.9%	9.9%	6.8%	6.3%	6.6%	5.6%	6.5%	5.4%	6.0%
	C(a _n)	3.46	2.63	2.18	2.0	3.03	5.22	3.02	2.52	2.93	3.44	5.58	5.86	5.54	4.88	4.25	3.39
	K(a _n)	2.35	2.41	2.53	2.37	1.61	1.66	2.09	2.54	2.65	2.23	2.06	2.08	2.17	2.29	2.33	2.68
Fukuoka (24.4 m)	A(a _n)	4.7%	2.2%	1.5%	2.0%	3.9%	16.4%	8.8%	5.1%	5.7%	4.8%	2.8%	4.6%	5.3%	4.6%	13.1%	14.7%
	C(a _n)	3.37	2.73	2.36	2.04	1.97	2.25	2.03	2.17	2.23	1.77	2.49	3.51	4.02	3.41	4.25	4.66
	K(a _n)	1.70	1.60	1.53	1.82	1.95	2.06	1.71	1.45	1.60	2.09	1.81	1.94	1.96	1.73	2.15	2.03
Sendai (52.0 m)	A(a _n)	4.0%	2.7%	1.7%	2.2%	5.0%	10.8%	8.7%	6.5%	3.7%	3.1%	3.1%	6.7%	9.7%	9.7%	13.0%	9.2%
	C(a _n)	2.63	2.12	1.88	1.75	2.22	3.56	3.65	3.19	2.70	2.51	3.27	4.65	5.50	4.24	3.56	3.70
	K(a _n)	1.80	1.80	1.67	1.55	1.82	2.03	1.89	1.91	1.83	1.89	1.64	1.64	1.68	1.76	2.14	1.92
Nagoya (17.9 m)	A(a _n)	5.1%	3.2%	2.6%	1.6%	2.6%	6.5%	8.6%	4.5%	2.3%	1.8%	1.6%	2.2%	9.4%	15.8%	19.3%	12.7%
	C(a _n)	1.98	1.73	1.73	1.46	2.11	3.16	4.00	3.46	2.66	2.57	2.53	3.21	4.79	4.44	3.31	2.53
	K(a _n)	2.53	2.45	2.41	2.17	1.98	2.08	2.12	2.13	2.22	2.12	1.95	1.71	2.11	2.04	2.27	2.51
Yokohama (19.5 m)	A(a _n)	9.2%	3.7%	4.1%	8.1%	5.2%	3.5%	3.6%	5.3%	7.0%	10.0%	3.9%	1.5%	0.9%	1.0%	5.3%	27.6%
	C(a _n)	3.17	2.35	2.92	3.43	2.86	2.75	3.65	3.96	4.91	5.48	4.56	2.83	2.72	2.75	3.70	4.44
	K(a _n)	2.73	2.89	2.55	2.84	3.00	2.64	2.10	2.37	2.20	2.28	1.94	2.04	2.00	1.85	2.49	2.57
Kyoto (16.1 m)	A(a _n)	11.0%	8.1%	5.7%	4.2%	2.4%	2.4%	3.4%	5.2%	6.1%	4.9%	5.3%	5.6%	7.8%	6.5%	9.1%	12.2%
	C(a _n)	1.51	1.60	2.21	2.48	2.03	1.72	1.80	2.18	2.30	1.90	1.95	1.85	1.71	1.68	2.20	1.98
	K(a _n)	2.29	2.00	1.81	1.70	1.53	1.64	1.90	1.93	1.87	1.89	2.00	1.96	2.06	1.89	1.81	1.82

*The numbers in brackets refer to the observation height.

Graphical representations of the parameter $A(a_n)$ for the nine cities are given in Fig. 6. The Weibull parameters for these cities were estimated through the regression of the data of mean wind velocity which was measured every three hours for a period of 10 years starting from 1995 until 2004, and averaged over 10 minutes. Values of the Weibull parameters for the sixteen azimuth directions in the nine selected Japanese cities are given in Table 1 (see Ref. (25)).

Since the velocity measurement heights in the nine cities are not equal, a correction factor has to be applied. Considering Tokyo is the reference city, the correction factor is estimated as:

$$F = U_{Tokyo} \left(\frac{h_{city}}{h_{Tokyo}} \right)^{0.25} \tag{10}$$

where F is a correction factor, U_{Tokyo} is the reference velocity of Tokyo (i.e. 1 m/s), h_{city} is the reference height of the considered city (such as Osaka, Sapporo...etc), and h_{Tokyo} is the reference

height of Tokyo (i.e. 74.6 m).

3.3. Numerical simulations

Numerical simulations were carried out through the CFD code STAR-CD, based on a finite-volume discretization method. Steady state analysis was adopted and the Monotone Advection and Reconstruction Scheme MARS (Star-CD Methodology, 2004) was applied to the convective term, and the central difference scheme was used for the diffusion terms. The pressure/velocity linkage is solved via the SIMPLE algorithm (Patankar 1980) and the first order upwind scheme (UD) was considered in solving the scalar eq. (i.e. Eq. (13)). Although the UD scheme provides a considerable amount of numerical diffusion (Patankar 1980), it was chosen here because it provides a stable solution.

Since many real flows are anisotropic and the standard $k-\varepsilon$ model eqs. don't account for the anisotropy, a non-linear version of the $k-\varepsilon$ model was preferred to simulate the turbulence effects. In this study, the cubic high Reynolds number $k-\varepsilon$ model (Star-CD Methodology, 2004) was used because this model caters for the above defect by adopting non-linear relationship between Reynolds's stresses and the rate of strain.

In expectation of greater simulation accuracy, a structured grid system was used to simulate the

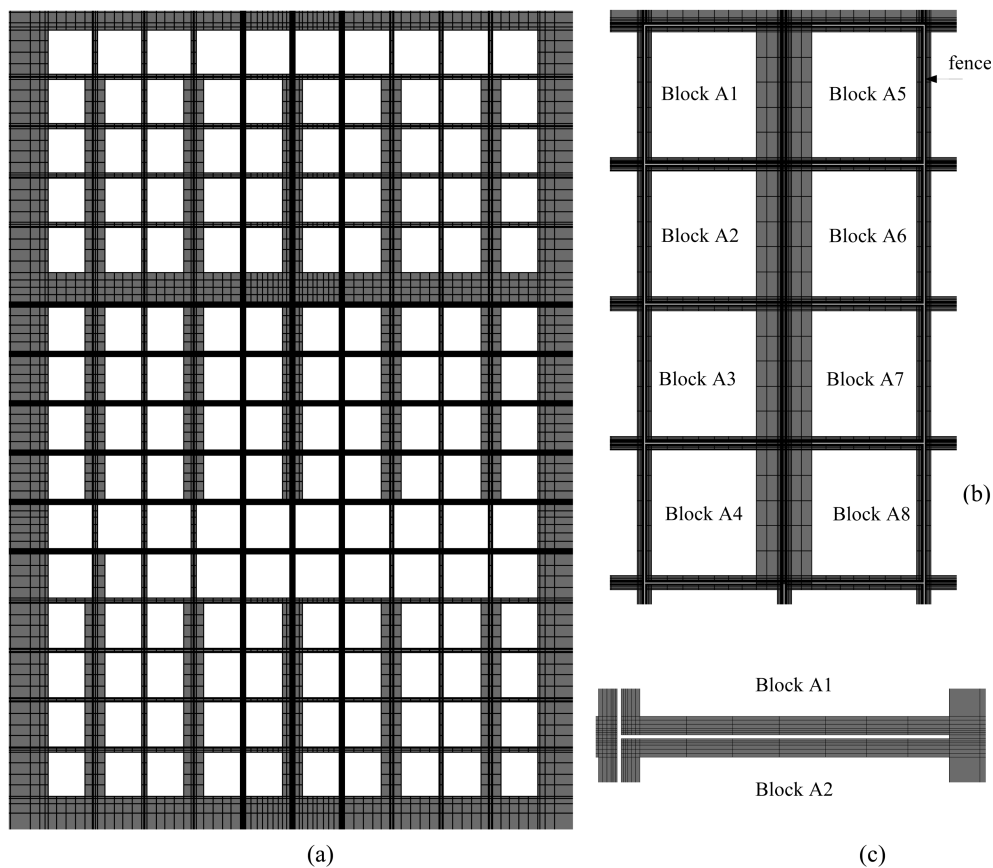


Fig. 7 Schematic representation of grid system to simulate the array of model (I); (a) grid system of the whole array; (b) grid system of the study domain; (c) grid system of the narrow passages between buildings

building arrays. Fine meshes were applied near the walls and around the buildings, and coarse ones were used far from them. In addition, as the passages between street buildings are a very important aspect for the simulation results, very fine meshes were used across the width of each passage, as mentioned by Blocken, *et al.* (2006). This arrangement was considered to ensure a proper resolution of the boundary layers and of the air flow in the study domain. Fig. 7 shows a schematic of the grid system for the building array of model (I) together with the grid characteristics of the study domain and the passages.

At the inflow boundary, a constant flux layer was assumed for the turbulent energy k , and turbulent intensity was assumed to be 10% of the inflow wind velocity at a representative height (z_o) of 74.6 m. The turbulent kinetic energy was calculated as given by Eq. (11), while the turbulent dissipation rate was calculated according to Eq. (12), which arises from the assumption of local equilibrium $P_k \cong \varepsilon$ (P_k : production term for k eq.) (Murakami, *et al.* (1988), Mochida, *et al.* (2002) and Tominaga, *et al.* (2008)).

$$k \cong 1.5(u_o \times I)^2 \tag{11}$$

$$\varepsilon \cong C_\mu^{1/2} \times k \times \frac{\partial u}{\partial z} \tag{12}$$

where k is the turbulent kinetic energy (m^2/s^2), u_o is the reference wind velocity (m/s), I is the turbulent intensity of the applied flow, u is the wind velocity (m/s), ε is the dissipation rate and C_μ is a constant.

The sides and the top of the computational domain are modeled as slip walls (zero normal velocity and zero normal gradients of all variables). The generalized logarithmic law with the parameter $E = 9$ (m) was applied to the building walls and ground surface as smooth walls. Table 2 summarizes the parameters used in the simulations together with the applied boundary conditions.

A uniform generation rate of the pollutant within the study domain is considered to be independent of the source location within the domain. The feature of applying uniform generation is that it is not necessary to consider the location of the pollutant source within the study domain. Then, pollutant concentration was calculated through the solution of the convective-diffusion eq. for a scalar (Ferziger, *et al.* 1997):

$$\frac{\partial(\rho u_i C)}{\partial x_i} = \frac{\partial}{\partial x_i} \left(K \frac{\partial c}{\partial x_i} \right) + S \tag{13}$$

Table 2 CFD simulation parameters together with applied boundary conditions

Turbulent Model	The cubic k - model
Differential schemes	MARS Scheme (Star-CD Methodology, 2004) Diffusion term: Central difference scheme Concentration: First order upwind scheme (UD)
Inflow conditions	$u = u_o(z/h_o)^{0.25}$, $u_o = 1$ m/s & $h_o = 74.6$ m $k = 1.5(u_o \times I)^2$, $I = 0.10$ $\varepsilon = C_\mu^{1/2} \times k \times \frac{\partial z}{\partial z}$, $C_\mu = 0.09$
Outflow conditions	Zero normal derivatives
Side and top boundaries	Free slip
Building walls and ground	Generalized logarithmic law ($E = 9$)

where c denotes pollutant concentration (kg/kg), K is the diffusivity coefficient for the concentration (kg/m²/s), x_i are the Cartesian coordinates (m), u_i are the Cartesian components of the velocity (m/s), and S is the pollutant source strength (kg/m³/s).

An important issue to be mentioned here is related to the diffusivity coefficient K which is a function of the turbulent Schmidt number ($K = \nu_t / Sc_t$). It is known that the numerical results are quite sensitive to the value of the turbulent Schmidt number (Blocken, *et al.* 2008). In addition, the value of Sc_t is not constant and varies from one location to another within the same calculation domain. In high concentration regions – which mean high concentration gradients – the turbulent Schmidt number is less than one, while in low concentration regions – which means that the mixing of pollutants with ambient fluid is almost finished – its value is sometimes greater than one. This means that the diffusivity coefficient does not equal the eddy diffusivity of the momentum. In order to determine the optimum value of Sc in urban areas through the regression of the observed data, a lot of studies have been carried out, such as Tominaga, *et al.* (2007), Moriguchi, *et al.* (1995) and Yoshikawa, *et al.* (1997). In these studies, it was found that $Sc < 1$ has good regression. Accordingly, in the present work, the turbulent Schmidt number was assumed to be constant and its value is the default value of STAR-CD which is 0.9 (Star-CD Methodology, 2004). The assumption of constant Schmidt number has been applied in many of the previous studies, such as Xiaomine, *et al.* (2005) and Tsai, *et al.* (2004), and gave reasonable results.

It is worth mentioning here the fact that the numerical simulation for diffusion is sometimes not accurate. This can be attributed to two main reasons – the insufficient spatial resolution and the steep concentration gradients that exist within the same calculation domain. This steep gradient is explained as follows: in the upwind side of a source, the concentration is zero; while in the region closest to the source, the concentration is a maximum and decreases as the plume travels downwind of the source. Accordingly, there is a significant variation in the concentration values between the adjacent cells, which leads to steep concentration gradients. In order to overcome these two problems, a huge number of cells is needed to produce gradual concentration gradients, which is computationally expensive. In this paper, in order to overcome the problem of insufficient spatial resolution, a grid-convergence analysis has been carried out during the design of the mesh systems of the three building models and in each case; a reasonable number of cells was attained.

Dimensions of the wind environment domain around the building arrays were not fixed. It was varied according to the applied wind direction. For example; when the wind direction was normal to the street (i.e. $\theta = 0^\circ$) the domain dimensions were 430 m×220 m (796589 cells), and when the wind angle was 315° , the domain dimensions were 430 m×420 m (872045 cells)...etc. However, the domain height was 82 m for all cases.

3.4. Wind tunnel experiments

Since the exceedance probability is calculated based on CFD simulations. So, it is very important to demonstrate that the numerical results are accurate. Thus, wind tunnel experiments were carried out to validate the calculated flow fields through measuring wind velocity and pollutant concentrations. These experiments were performed in the boundary layer wind tunnel of the University of Tokyo. In such experiments, the building patterns were represented by 1:100 scale wooden models and wind velocity and tracer gas concentrations were measured along the two sides of the street over an extended range of incident wind directions. Six directions have been considered and applied to each model. These directions were: 0° , 22.5° , 45° , 90° , 270° , and 315° . In each case,

wind velocities and tracer gas concentrations were recorded along the two sides of the street at 1.5-m height. For more details about the experiments, see Bady, *et al.* (2008).

4. Results and discussion

4.1. Comparison between numerical and experimental results

Some examples for comparing CFD simulation results with the experimental data for wind velocity at three levels of $z = 1.5$ m, 3.0 m and 9.0 m are presented in Figs. 8-10. Fig. 8 (a) shows the wind velocity in the region $y = 0\sim 40$ m along the two sides of the street of model (I) at 1 m apart from the street center line. In the subplot (a), the calculated and the measured scalar velocities along the left hand side of the street ($X = -1$ m) at the three considered heights is shown. In numerical and experimental approaches, a general observation can be noticed that the velocity tends to increase from the inner end of the street ($y = 0$ m) to its open end ($y = 40$ m), which is located alongside the traffic road. Also, the figure shows satisfactory agreements between the numerical and experimental results along the inner half of the street ($0 \leq y \leq 20$) at $z = 1.5$ m and $z = 3.0$ m.

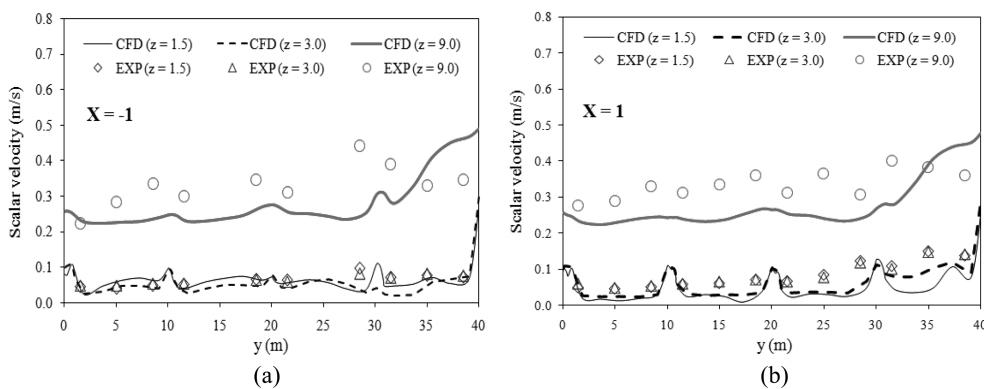


Fig. 8 Comparison between numerical and experimental wind velocities along the sides of the street of model (I) at $\theta = 0^\circ$; (a) $X = -1$ m, and (b) $X = 1$ m

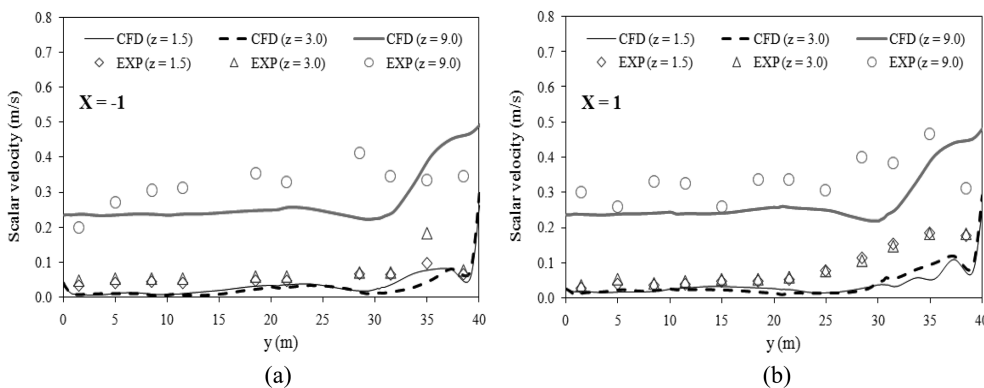


Fig. 9 Comparison between numerical and experimental wind velocities along the sides of the street of model (II) at $\theta = 0^\circ$; (a) $X = -1$ m, and (b) $X = 1$ m

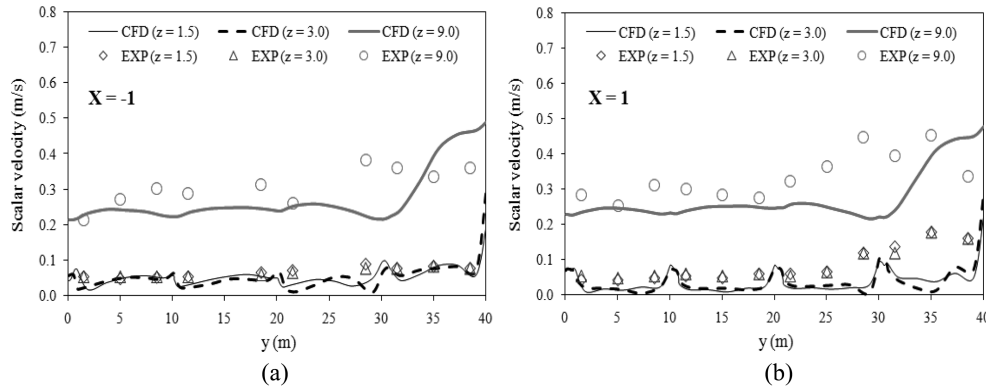


Fig. 10 Comparison between numerical and experimental wind velocities along the sides of the street of model (III) at $\theta = 0^\circ$; (a) $X = -1$ m, and (b) $X = 1$ m

However, a considerable difference is observed along the second half of the street ($20 < y \leq 40$). These differences could be attributed to the fact that the measurement points near the traffic road ($y = 40$ m) are in locations of highly complex circulatory flow regions. In the same time, there are peak values for the wind velocity along this side of the street for these two wind directions near the narrow spaces between the street buildings. This behavior reflects the importance of the presence of such spaces between adjacent buildings to induce more wind through urban domains. Fig. 8(b) shows the wind velocities along the right hand side of the street ($X = 1$ m). Similar to the case of $X = -1$ m, good agreements are observed along the inner half of the street, while near the road side the differences between the two approaches are larger than those of the case of ($X = -1$ m). In Figs. 8(a) and 8(b), at $z = 9$ m, a large difference between the calculated and the measured velocities are shown. The velocities calculated by CFD simulation underestimate the measured velocities. This can be attributed to the shortage of the turbulence model in predicting the velocity gradient near building walls and roofs.

In Figs. 9 and 10, the similar comparisons of numerical predictions with the experimental results for models (II) and (III) in the two wind directions are shown, respectively. Similar to the results of model (I), the numerical predictions of the two models, overall, are in satisfactory agreement with the experimental results, but the major discrepancies are present at $z = 9.0$ m. In addition to the shortages of the $k-\varepsilon$ model in predicting the velocity gradient near walls and roofs, the computational errors include the inaccuracies introduced by the discretization scheme, parameter selection, and algebraic eq. solutions. In general, however, the overall agreement between numerical predictions and experimental measurements is good.

4.2. Air exchange rate within the study domain

Fig. 11 shows the air quality parameters: average pollutant concentration and air exchange rate, within the pedestrian domain of the street for the three building patterns versus the applied wind direction. Such quantities were estimated at a reference wind velocity of 1 m/s measured at a reference height of 74.6 m.

The results demonstrate a significant dependence on the wind direction and also on the building array geometry. In the range from $0 \sim 180^\circ$, models (I) demonstrate good ventilation performance

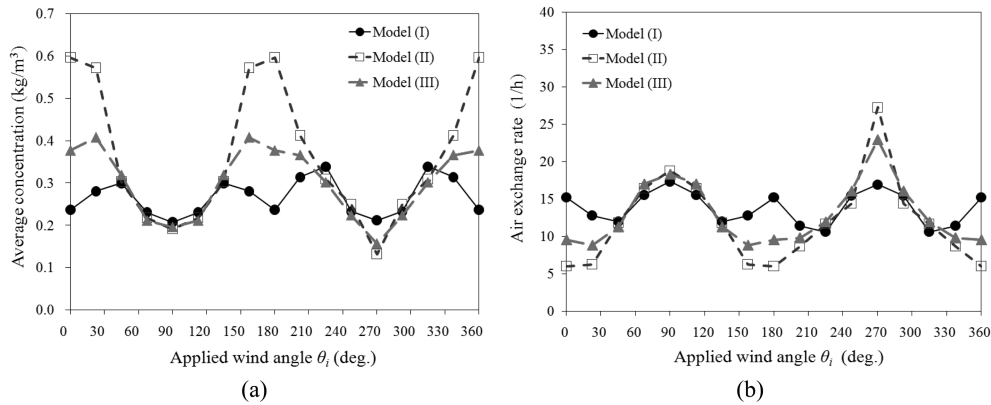


Fig. 11 Air quality parameters within the study domain for the three patterns ($u_o = 1$ m/s); (a) Average domain concentration, (b) Air exchange rate

compared with the other models. The behavior of such model for this wind direction range reflects the high removal efficiency of the pollutants by the wind, which is attributed to the presence of narrow gaps between street buildings. The narrow gaps induce more wind to the street domain, which improves the ventilation process. The effect of these gaps clearly appears in the case of model (III) also, which demonstrates good performance compared with model (II), which has the lowest ventilation performance among the three models in this range of wind directions. It is thought that the geometry of the solid U-shape in model (II) and the outer U-shape of model (III) are the main reasons for these trends in this range of wind directions. The U-shaped geometry prevents the removal of pollutants by the applied wind in specific wind directions, which leads to an increase in the returning flux of these pollutants to the domain. The pollutants then accumulate and the concentration increases.

In the range from $\theta_i = 180^\circ \sim 360^\circ$, models (II) and (III) clearly demonstrate high ventilation performances. The effect of wind direction in such range can be understood by realizing that most of the wind which enters the street domain comes through the shear layer at building roof level, while a low percentage of wind enters the domain through the traffic road side and the narrow gaps between street buildings. The wind flow through the narrow gaps creates lateral flows, which appear clearly in model (I) compared with model (III), while these flows disappear completely in the case of model (II). The interaction between these flows and the main flow coming across the shear layer creates a number of vertices within the street, which affect the purging capability of the main flow.

4.3. Application of exceedance probability

Results of calculating the exceedance probabilities within the study domain for the case of model (I) are presented in Fig. 12. In order to maintain the brevity of this paper, among the nine cities considered, only the probability curves of three cities are presented. These cities are: Tokyo, Sapporo and Yokohama. For each city, there are sixteen curves representing the sixteen directions considered for the building arrays. Each curve represents the total exceedance probability for the considered direction of the array. For example, the curve of NW-direction represents the total exceedance probability from the sixteen wind directions when the array direction is NW.

The figure shows that at higher exceedance probabilities, the difference between *AER* values from

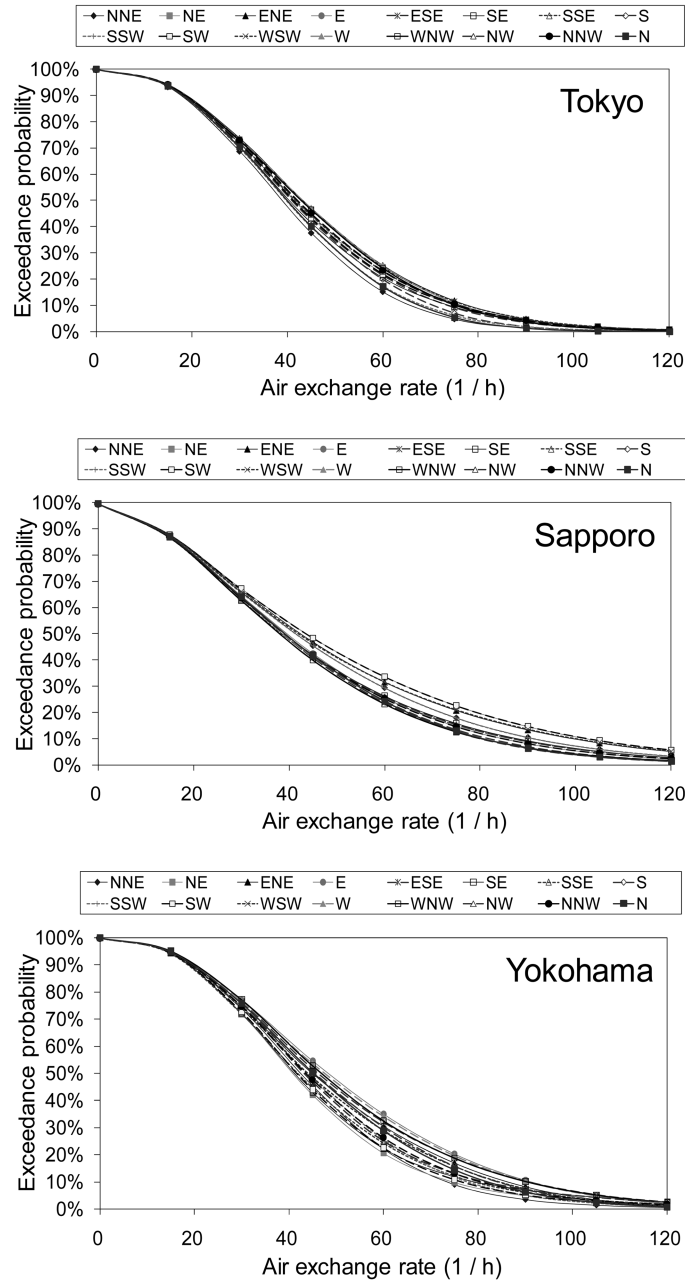


Fig. 12 Exceedance probability curves of model (I) in Tokyo, Sapporo and Yokohama

one direction to another is very small, while at low probability values, such differences are considerable. For example, in the case of Tokyo, at a probability value of 70%, the *AER* is about 30 1/h in almost all directions of the array with no considerable differences between these directions. However, at an exceedance probability of 20%, the *AER* ranges from 50 1/h in the NNE direction to 65 1/h in the W direction. Also, the figure demonstrates that for a specific air exchange rate and a

specific array direction, the probability values vary from one city to another due to the variation of the wind characteristics between these cities. In addition, the figure demonstrates the low dependence of model (I) on the array direction for almost all cities. This appears clearly in the convergence between the probability curves in the sixteen directions of the array. This means that the change in *AER* is very small with changes in the array direction in these kinds of densely urban areas. Another important point to note from this figure is that model (I) has low probability values at higher ventilation rates in Tokyo. This can be attributed to the wind characteristics of Tokyo, reflected by the values of the parameters $C(a_n)$ and $K(a_n)$.

The results of Fig. 12 demonstrated that it is difficult to evaluate the calculated exceedance probabilities for all 16 directions due to the high density of the curves. Accordingly, it was preferred here to compare the ventilation performance of the three building models based on specific values of air exchange rate.

4.3.1. Assessment of wind conditions based on *AER*

Fig. 13 shows the exceedance probabilities of the three building patterns within the study domain for the considered nine cities. The sixteen model directions -starting from N to NNW in a clockwise rotation- are signed with numbers from 0~15 and used as the horizontal axis in such figure. The air exchange rate was considered as the key parameter and it is changed from 15 1/h to 120 1/h with a step of 15 1/h. The limited number for the values of *AER* is considered here since it is impossible to show the whole range on the same graph.

The exceedance probability distribution of Tokyo is shown in Fig. 13(a). At *AER* = 15 1/h, the probability trends are almost constant for models (I) and (III) at a probability value of about 90%, while model (II) shows little variation with model direction. The variation of the exceedance probability with the model direction becomes large as the air exchange rate increases, where the significant difference between the maximum and the minimum probabilities are occurred at *AER* = 60 1/h, which is the same at almost all cities.

Fig. 13(d) shows the exceedance probability curves of Niigata. In such case, the probability trends are shifted up compared with the other cities due to the strong wind of Niigata. In the same subplot, the exceedance probability at air exchange rate of 120 1/h is shown too. For this value, the exceedance probability is about 5%. The probability trends of Niigata demonstrate that; the variation of the probability with the model direction is fairly large. The variation of exceedance probability with model direction at *AER* of 120 1/h is still greater than that of Yokohama shown in Fig. 13(h). Similarly, the variation of the exceedance probability with the model direction at the specific air exchange rates of the other cities can be read from Fig. 13.

4.3.1.1. Influence of building geometry on exceedance probability distribution

In order to investigate the influence of the three building models on the ventilation performance within the study domain, the case of *AER* = 60 1/h is focused here. In the case of model (I), the exceedance probability variation with the array direction is the lowest among the three models. This reflects the influence of the 1 m space between the adjacent buildings in achieving high ventilation performance of the applied wind. Model (II) is a series of adjacent buildings where no space exists. The exceedance probability variation with the array direction is very large, where the difference between the maximum and the minimum probabilities at certain cities exceeds 30%. With respect to model (III) which is a model that the detached houses are surrounded by a series of building, the

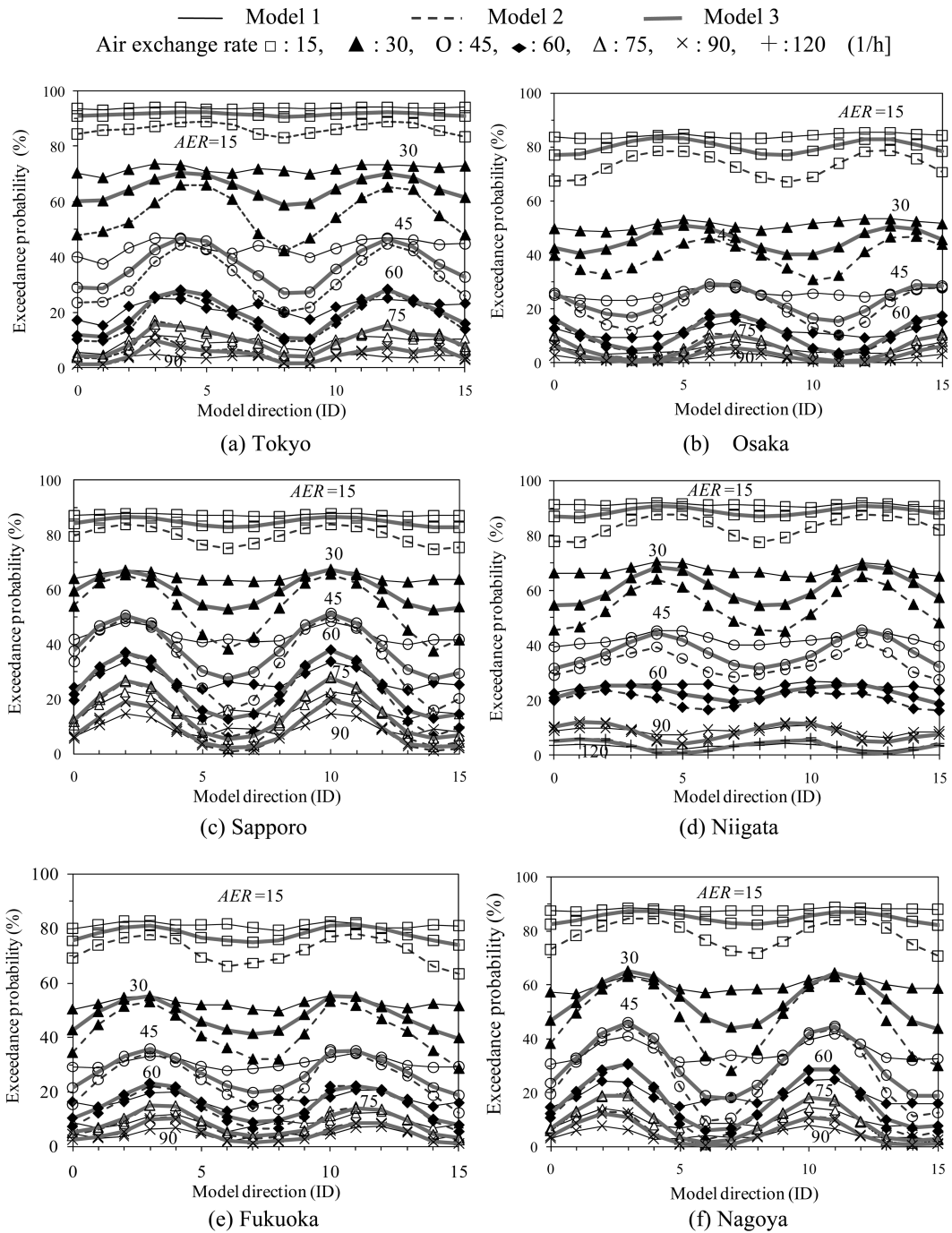


Fig. 13 Exceedance probabilities within the domain for the three building models in the nine cities

variation of the exceedance probability with the array direction is in-between models (I) and (II) in almost all cities.

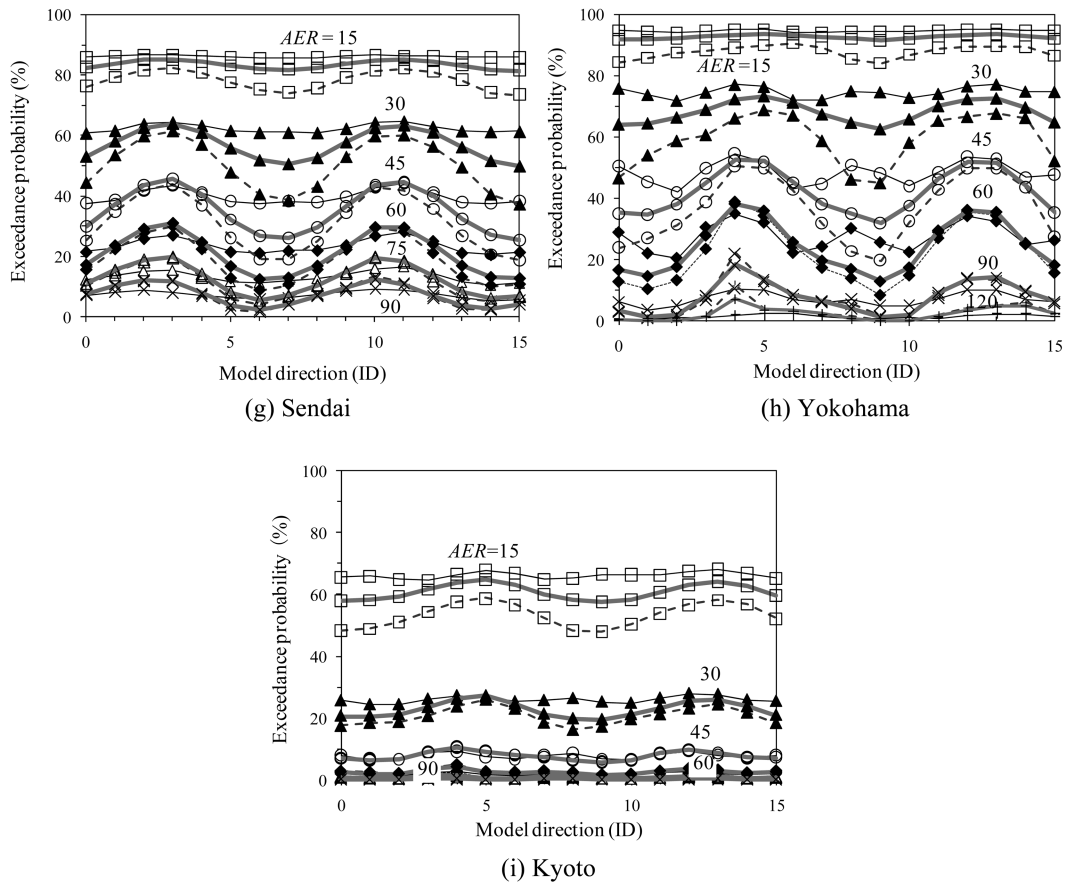


Fig. 13 Continued.

4.3.1.2. Comparison between the exceedance probabilities of the nine cities

Fig. 14 presents a comparison between the exceedance probabilities of the nine cities within the study domain for the three building patterns. The figure shows the maximum and the minimum exceedance probability trends estimated at an air exchange rate of 60 1/h. Also, the figure shows the directions at which these probabilities were calculated.

Fig. 14 (a) shows the maximum and the minimum probability trends of Tokyo. In such figure, the difference between the maximum and the minimum probabilities of model (I) (difference between □ and ■) is small, while such difference becomes large in the case of model (II) (difference between ▲ and △). Although, model (III) shows a behavior between the two models (difference between ○ and ●), it demonstrates the highest probability values among the three models. In Fig. 14 (d), it is clear that the differences between the maximum and the minimum probabilities become smaller in Niigata compared with Tokyo which is attributed to the wind rose of the two cities. Referring to Fig 6, the wind rose of Tokyo has two peaks at NNW and SW, while that of Niigata is almost forming an oval. This means the sensitivity of the probability to wind direction in Tokyo is larger than that of Niigata. In addition, the slope of the probability trends of Tokyo is larger than Niigata. This is attributed to the distribution of the Weibull parameter C_n , which has the same units of velocity according to Eq. (10). The greater the value of C_n , the smaller the slope of the trends

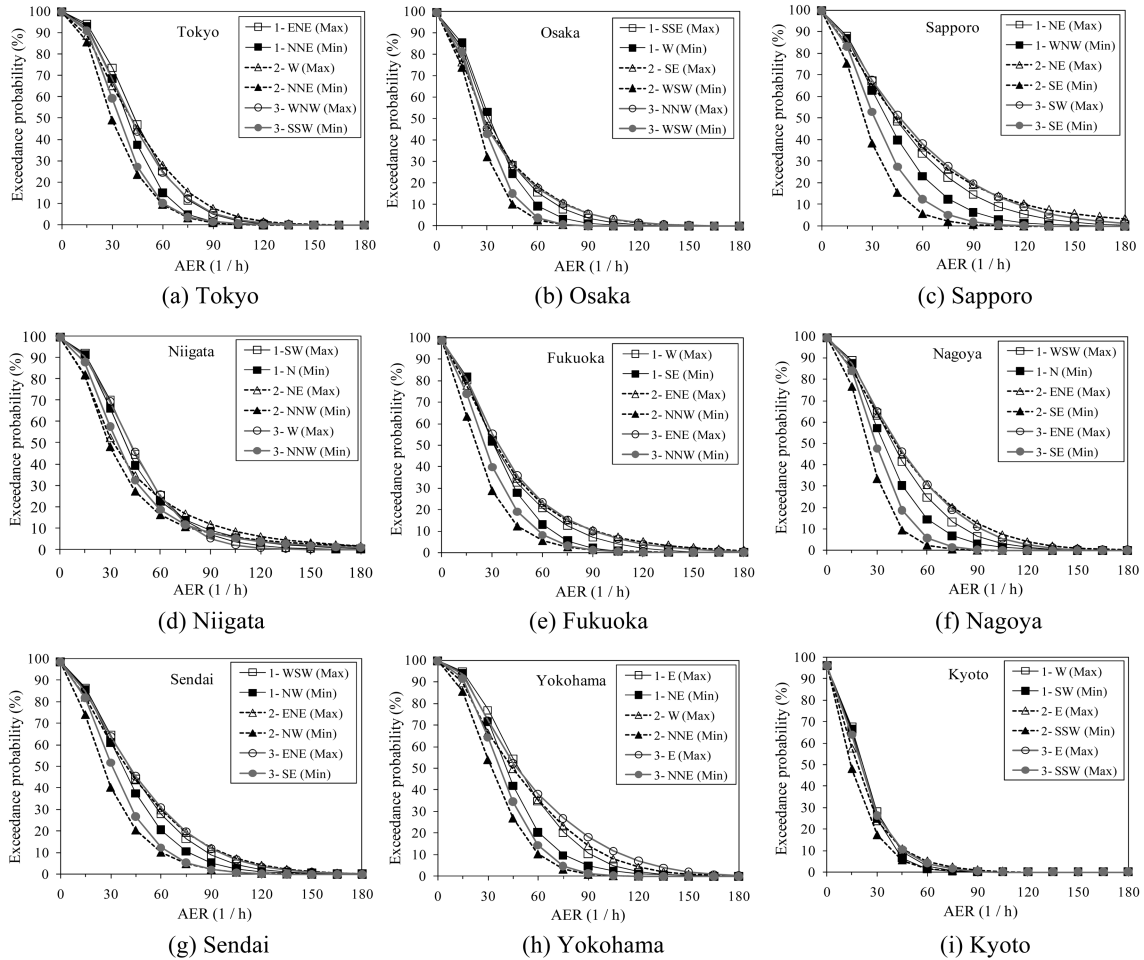


Fig. 14 Maximum and minimum 60 times/h air exchange rate -based exceedance probability for the three models in the nine cities together with the model directions of each case

(and vice versa). In Tokyo, the parameter C_n is almost distributed on a circle while that of Niigata is not uniform and its values are greater than Tokyo.

For the case of Nagoya -shown in Fig. 14(f) - the differences between the probability trends of the three models are greater than those of Yokohama. This can be referred to the wind distribution along the wind rose, which is concentrated on the NNW-SSE axis. Also, the parameter C_n of Nagoya is distributed on an oval and its values are lower than those of Yokohama. This gives a gradual decrease for the probability trends in Yokohama compared with Nagoya.

Fig. 14(c) shows the probability trends of Sapporo. In such case, the differences between the maximum and minimum probability trends of the three building patterns are smaller than those of Nagoya. Similar to Nagoya, the main wind direction in Sapporo is concentrated along the NW-SE axis which makes the wind characteristics in these two directions differ greatly from the other directions. The figure shows also that; the slopes of the probability curves are almost the same as those of Nagoya, since the distribution of the parameter C_n in the two cities is nearly the same.

With respect to case of Kyoto, shown in Fig. 14(i), the applied wind intensity is quite low in all directions as shown in Fig. 6(i). Thus, the difference between the maximum and the minimum probability curves of the models are small (see Fig. 13(i)). Also, since the parameter C_n is almost distributed on a circle, the slope of the trends is quite large.

From the above discussion, it is clear that; when the wind ventilation performance in a certain area is investigated, the wind rose of such area is very important for reflecting its wind characteristic. The wind rose reflects the behavior of the incident wind at a certain direction for the 16 model directions. This means that; Fig. 6 together with Fig. 14, are important to study the wind performance in built-up areas.

4.3.1.3. Assessment based on 85% and 15% exceedance probabilities

In order to assess the wind conditions of the three building patterns in the nine cities based on the calculated exceedance probabilities, a reasonable measure is required. This measure should exhibit a time relevance of a repeating nature. Accordingly, it is adopted here to use the wind occurrence of a week as a base of comparison. One day per week reflects a probability of occurrence of 15% ($1/7 = 0.1428 \approx 15\%$) and six days per week reflect a probability of occurrence of 85% ($6/7 = 0.857 = 85\%$). So, the investigation of *AER* values at these two probabilities will be informative.

Table 3 presents the values of *AER* for the three building patterns in the nine cities at $P = 85\%$ and 15%. As an example, consider the case of model (I) in Tokyo. According to Table (3), it is

Table 3 *AER* values at the exceedance probabilities of 15% and 85% together with models directions

City	Model (I)		Model (II)		Model (III)	
	85%	15%	85%	15%	85%	15%
Tokyo	SSW	W	ESE	W	NNE	W
	28.57	69.45	20.25	71.66	27.77	71.68
Osaka	W	SE	WNW	SE	E	NW
	15.36	57.52	10.4	55.1	13.57	56.55
Sapporo	ENE	NE	NW	ENE	NNW	SW
	18.82	78.99	24.13	71.79	16.35	76.00
Niigata	ENE	E	E	W	ESE	W
	25.39	68.62	18.17	65.83	23.31	69.35
Fukuoka	NE	WSW	WSW	SW	NNW	ENE
	12.92	63.23	9.95	64.52	11.85	64.38
Nagoya	W	WSW	E	ENE	ESE	ESE
	21.41	67.49	14.48	71.07	17.74	71.99
Sendai	SW	WSW	ENE	ENE	ENE	ENE
	17.22	70.08	12.50	70.42	14.96	71.86
Yokohama	SE	E	SE	W	SSE	W
	28.75	79.46	23.8	76.69	28.07	78.19
Kyoto	WNW	WNW	ESE	ESE	ESE	ESE
	5.99	46.80	4.49	42.04	5.34	44.92

expected that the air exchange rate within the pedestrian domain of model (I) will be more than 28 1/h for six days/week, and more than 69 1/h for one day/week. Also, in the case of Kyoto, the number of air changes can be expected to be about 46 1/h for one day/week, and more than 6 1/h for six days/week. Clearly, these rates are quite lower than those of Tokyo. Another example is the case of Sapporo. In such case, the air exchange rate will be more than 18 1/h for six days/week which is lower than Tokyo and more than 79 1/h for one day per a week which is greater than Tokyo. This can be attributed to the fast decay of the probability curves in Sapporo at low *AER* values and also to the gradual decrease of the probability curves of Sapporo compared with Tokyo at high *AER* values, according to Fig. 14.

Moreover, based on Table 3, the lowest *AER* values within the study domain for the three models are found in Kyoto at both $P = 85\%$ and 15% , while the highest values float between Yokohama, Sapporo and Niigata. This note demonstrates that the wind conditions in these tree cities are better than those of the other cities, even in weak wind conditions. In addition, the table demonstrates that model (II) has the lowest *AER* values among the three models, while models (I) and (III) show nearly the same *AER* values. Since the minimum standard values of the air exchange rate within these cities are not exactly determined in the present stage of this study, it is difficult to state that model (II) is unacceptable.

5. Conclusions

Three typical models of a dense urban area were studied and numerically simulated to examine the effects of the geometry of these building patterns on wind flow characteristics within the pedestrian domain of a street located within this area. The exceedance probability was considered to assess the performance of the wind environment of the three models. A new approach for calculating the exceedance probability was introduced based on air exchange rate within the study domain as a reflection of air quality. The study was applied to nine cities in Japan, based on their mean wind velocity data. The study revealed the following:

- 1) The exceedance probability seems to be an effective tool for evaluating wind conditions within urban domains. It affords the ability to estimate the optimum direction for building arrays that provide a good wind environment for inhabitants of such areas by improving the air quality.
- 2) Dense building arrays with some narrow gaps can be set in any direction within the construction site. The presence of narrow gaps leads to a decrease in differences between air exchange rates for variable wind directions.
- 3) Since the study target is to assess the wind environment of the building arrays in nine selected Japanese cities, the wind conditions of Yokohama, Sapporo and Niigata seem to be better than those of the other cities, reflected by the *AER* values at the minimum probability values. This conclusion is drawn from the weak wind point of view.
- 4) The exceedance probabilities strongly depend on the geometries of the building arrays as well as the wind conditions of the construction site.

References

- Bady, M., Kato, S., Takahashi, T. and Huang, H. (2008), "A study on ventilation in densely populated urban areas, an experimental investigation of pedestrian wind environment and air quality within an urban street canyon", Submitted.

- Bady, M., Kato, S. and Hong, H. (2008), "Towards the application of indoor ventilation efficiency indices to evaluate the air quality of urban areas", *Build. Environ.*, **43**(12), 1991-2004.
- Blocken, B. and Carmeliet, J. (2008), "Pedestrian wind conditions at outdoor platforms in a high-rise apartment building: generic sub-configuration validation, wind comfort assessment and uncertainty issues", *Wind Struct.*, **11**(1), 51-70.
- Blocken, B., Roels, S. and Carmeliet, J. (2004), "Modification of pedestrian wind comfort in the Silvertop tower passages by an automatic control system", *J. Wind Eng. Ind. Aerodyn.*, **92**, 849-873.
- Blocken, B., Stathopoulos, T. and Carmeliet, J. (2006), "Towards grid resolution guidelines for CFD simulations of wind speed in passages between buildings", *The Fourth International Symposium on Computational Wind Engineering (CWE2006)*, 117-120, Yokohama, Japan.
- Blocken, B., Stathopoulos, T., Saathoff, P. and Wang, X. (2008), "Numerical evaluation of pollutant dispersion in the built environment: Comparisons between models and experiments", *J. Wind Eng. Ind. Aerod.*, **96**(10-11), 1817-1831.
- Ferziger, J. and Peric, M. (1997), *Computational Methods for Fluid Dynamics*, Second Edition, Springer, Germany.
- Huang, H., Ooka, R., Kato, S. and Jiang, T. (2006), "CFD analysis of ventilation efficiency around an elevated highway using visitation frequency and purging flow rate", *Wind. Struct.* **9**(4), 297-313.
- Isumov, N. and Davenport, A.G. (1975), "The ground level wind environment in built-up areas", *Proceedings of Fourth International Conference of Wind Effect on Buildings and Structures*, 403-422.
- Katsumata, W. (2004), "Strategies for improving the residential environment of existing suburban small-lot residential areas through harmoniously controlling the rebuilding of houses", PhD Thesis, The University of Tokyo, Japan (in Japanese).
- Melbourne W. (1978), "Wind environment studies in Australia", *J. Ind. Aerodyn.*, **3**(2-3), 201-214.
- Melbourne, W. (1978), "Criteria for environmental wind conditions", *J. Ind. Aerodyn.*, **3**(2-3), 241-249.
- Mochida, A., Tominaga, Y., Murakami, S., Yoshie, R., Ishihara, T. and Ooka, R. (2002), "Comparison of various k- ϵ models and DSM applied to flow around a high-rise building- report on AIJ cooperative project for CFD prediction of wind environment", *Wind Struct.*, **5**(2-4), 227-244.
- Moriguchi, M., Matsuoka, Y. and Harasawa, H. (1995), "A finite difference model for automotive exhaust gas dispersion near urban roadways (I) Calculation scheme and two dimensional model for cross wind", *J. Jap. Soc. Air Pollut.*, **30**, 1-19 (in Japanese).
- Murakami, S. (1983), "Turbulence characteristics of wind flow at ground level in built-up area", *J. Ind. Aerodyn.*, **15**, 133-144.
- Murakami, S. (1986), "Study on acceptable criteria for assessing wind environment at ground level based on residents' diaries", *J. Wind Eng. Ind. Aerodyn.*, **24**(1), 1-18.
- Murakami, S., Mochida, A. and Hayashi, Y. (1988), "Modification of production terms in k- ϵ model to remove overestimate of k value around windward corner", *The Tenth Wind Engineering Symposium of Japan*, 199-201, (in Japanese).
- Ohba, S., Kobayashi, N. and Murakami, S. (1998), "Study on the assessment of environmental wind conditions at ground level in a built-up area -based on long-term measurements using portable 3-cup anemometers", *J. Wind Eng. Ind. Aerodyn.*, **28**(1-3), 129-138.
- Patankar, S. (1980), "Numerical heat transfer and fluid flow", Hemisphere Publishing Corporation, New York.
- Ratcliff, M. and Peterka, J. (1990), "Comparison of pedestrian wind acceptability criteria", *J. Wind Eng. Ind. Aerodyn.*, **36**(1-3), 791-800.
- Richards, P., Mallinson, G., McMillan, D and Li, Y. (2002), "Pedestrian level wind speeds in downtown Auckland", *Wind. Struct.*, **5**(2-4), 151-164.
- STAR-CD, Methodology, STAR-CD, Version 3.22 (2004), Computational Dynamics Limited.
- Stathopoulos, T. (2006), "Pedestrian level winds and outdoor human comfort", *J. Wind Eng. Ind. Aerodyn.*, **94**, 769-780.
- Tominaga, Y., Mochida, A., Yoshie, R., Kataoka, H., Nozu, T., Yoshikawa, M. and Shirasawa, T. (2008), "AIJ guidelines for practical applications of CFD to pedestrian wind environment around buildings", *J. Wind Eng. Ind. Aerodyn.*, **96**(10-11), 1749-1761.
- Tominaga, Y. and Stathopoulos, T. (2007), "Turbulent Schmidt numbers for CFD analysis with various types of flowfield", *Atmos. Environ.*, **41**(37), 8091-8099.

- Tsai, M. and Chen, K. (2004), "Measurements and three-dimensional modeling of air pollutant dispersion in an urban street canyon", *Atmos. Environ.*, **38**(35), 5911-5924.
- Visser, G. and Cleijne, J. (1994), "Wind comfort predictions by wind tunnel tests: comparison with full-scale data", *J. Wind Eng. Ind. Aerodyn.*, **52**, 385-402.
- Wind Engineering Institute of Japan (2005), *Fundamentals of Wind around Buildings*, Kajama Publisher.
- Xiaomine, X., Huang, Z. and Wang, J. (2005), "Impact of building configuration on air quality in street canyon", *Atmos. Environ.*, **39**(25), 4519-4530.
- Yoshikawa, Y., Kunimi, H. and Ishizawa, S. (1997), "Numerical simulation model for predicting air quality along the urban main roads: (I) Development of atmospheric diffusion model", *J. Jap. Mech. Soci.*, **63**, 2507-2514 (in Japanese).

CC